

# Development and physicochemical characterization of solid lipid nanoparticles containing tinidazole

Ho Hoang Nhan<sup>1\*</sup>, Le Thi Thanh Ngoc<sup>1</sup>, Le Hoang Hao<sup>1</sup>, Tran Thi Kieu Ny<sup>1</sup>, Dao Anh Tuan<sup>1</sup>

(1) Faculty of Pharmacy, Hue University of Medicine and Pharmacy, Hue University

## Abstract

**Background:** Periodontitis is a chronic inflammation of the periodontal tissues. To increase the effectiveness of treatment, antibiotics selected should have a spectrum of action on bacteria causing periodontitis, while also meeting the requirements of cell penetration and prolonging of the retention time at the target site. Therefore, this study aimed at developing solid lipid nanoparticles (SLNs) containing tinidazole (TNZ-SLNs) oriented to be incorporated into the gel to increase the penetration ability and prolong drug retention time in periodontal tissues. **Objectives:** Therefore, this study aimed to develop and characterize solid lipid nanoparticles (SLNs) containing tinidazole (TNZ-SLNs) oriented to be incorporated into the gel to increase the penetration ability and prolong drug retention time in periodontal tissues. **Methods:** TNZ-SLNs were prepared by combining hot homogenization and solvent evaporation using different types of lipids and surfactants. Factors related to the formula and the preparation process were investigated, Design Expert 12.0, FormRules v2.0 and InForm v3.1 software were used to design experiments and optimize the formula. The prepared nanoparticles were characterized by particle size, polydispersity index (PDI), encapsulation efficiency (EE), etc. **Results:** The optimized formulation had a particle size of  $197.60 \pm 19.67$  nm, a PDI of  $0.247 \pm 0.011$ , a zeta potential of  $-15.79 \pm 0.75$  mV and an EE of  $37.96 \pm 0.91\%$ . TNZ-SLNs showed prolonged in vitro drug release (for up to 24 hours), while TNZ material achieved about 100% drug release after 4 hours. **Conclusion:** TNZ-SLNs were successfully fabricated and physicochemically characterized.

**Keywords:** Tinidazole, solid lipid nanoparticles, periodontitis.

## 1. BACKGROUND

Periodontitis is a condition characterized by chronic inflammation in the periodontal tissues, occurring due to an imbalance between bacteria (mainly Gram-negative anaerobes) and the protective mechanisms in the periodontium. The use of local antibiotic therapy is advised because it provides a quick cure and reduces the negative effects of systemic antibiotic use. Tinidazole (TNZ), a 5-nitroimidazole antibiotic, is a second-generation drug derived from metronidazole. It exhibits excellent activity against gram-negative anaerobes and demonstrates higher sensitivity than metronidazole against anaerobic bacteria. In comparison to metronidazole, the oral administration of systemic TNZ for the treatment of periodontitis has proved to have a number of benefits [1].

Nanotechnology has attracted a lot of interest recently due to its excellent benefits for the pharmaceutical sector. Compared to traditional drug molecules, nanosized drug molecules improve therapeutic efficacy and boost absorption. Additionally, the advent of nanotechnology has been embraced by the pharmaceutical field as a

fundamental tool for researching and developing new drug delivery systems, such as localized drug delivery, sustained release, and targeted therapy. These advancements aim to overcome the limitations of conventional drugs and formulations, such as low solubility, poor bioavailability, wide distribution, while reducing the frequency of drug administration, enhancing treatment adherence, and improving patients' quality of life [2]. Among these approaches, solid lipid nanoparticles (SLNs) stand out as a promising direction. SLNs are nanosized particles composed of lipids in a solid state at room temperature dispersed in water or aqueous surfactant solutions. SLNs offer numerous outstanding advantages, including high biocompatibility, avoidance of allergic reactions, enhanced drug solubility, reduced toxicity, increased bioavailability, and improved cellular penetration. Due to these characteristics, they are ideal for targeted gel compositions used to treat periodontitis [2].

Thus, this study was aimed to formulate the SLNs containing TNZ (TNZ-SLNs) as well as evaluate some physico-chemical properties of the formulations.

Corresponding author: Ho Hoang Nhan, email: hhnhan@huemed-univ.edu.vn

Received: 22/2/2023; Accepted: 4/5/2023; Published: 10/6/2023

## 2. MATERIALS AND METHODS

### 2.1. Materials

Tinidazole (purity of 100%, European Pharmacopoeia 10) was obtained from Zhejiang Supor Pharmaceuticals Co., Ltd (China); Precirol ATO 5 and Compritol ATO 888 were purchased from Gattefossé (France); Poloxamer 407 was supplied by BASF (Germany); stearic acid, glyceryl monostearate (GMS), Tween 80, Cremophor RH40, dichloromethane (DCM), methanol (MeOH), hydrochloric acid (HCl) were obtained from China.

### 2.2. Methods

#### 2.2.1. Preparation and optimization of tinidazole - loaded solid lipid nanoparticles

Based on the preliminary studies, the hot homogenization method combining solvent evaporation was used to produce TNZ – loaded solid lipid nanoparticles (TNZ-SLNs). The lipid and TNZ (0.2% w/w) were melted at a temperature of 60 - 70°C in a solvent mixture (DCM:MeOH=3:1, v/v), while the appropriate amount of surfactant was added to 25 mL of water and heated to 70–80°C. The oil phase was added to the water phase under stirring at a rate of 1000 rpm and homogenized at an amplitude of 100W for 10 minutes (VCX-130, Sonics and Materials, USA), while the temperature was maintained at 70 - 80°C. Subsequently, the solvent was removed by vacuum evaporator (Buchi R-100, Switzerland).

For optimization study, the experimental design was conducted using Design Expert 12.0 software, employing a Box-Behnken design with 15 experiments. Analysis and optimization were performed to determine the influential factors and select the optimal formulation using FormRules v2.0 and InForm v3.1 software (Intelligensys Ltd, UK) based on an artificial neural network model.

#### 2.2.2. Characterization of tinidazole – loaded solid lipid nanoparticles

##### 2.2.2.1. Particle size and zeta potential analysis

The average particle size and polydispersity index (PDI) were measured by using the dynamic light scattering (DLS) method after dilution of an aliquot of nanoparticle (NP) suspension in distilled water (Zetasizer Nanoseries, Malvern Instruments, UK). The zeta potential values of the samples prepared for particle size analysis were determined by utilizing a folded capillary zeta cell.

##### 2.2.2.2. X-ray diffraction analysis

The XRD analysis of samples were performed with the X-ray diffractometer (D8 ADVANCE, Bruker, Germany) with a copper K $\alpha$  radiation ( $\lambda=1.5406 \text{ \AA}$ ), a reflection angle ( $2\theta$ ) ranging from  $10^\circ$  to  $70^\circ$ , a step size of  $0.02^\circ$ , a total measurement time of 498

seconds per step, a current of 40 mA, and a voltage of 40 kV. The measurements were conducted at a room temperature of  $25 \pm 2^\circ\text{C}$  [3]. The experiments were carried out on TNZ, excipients, a physical mixture of the components.

##### 2.2.2.3. Fourier Transform-Infrared (FTIR) spectroscopy analysis

FTIR spectra were obtained using an FTIR spectroscopy (Prestige-21, Shimadzu, Japan). The samples (TNZ, excipients, physical mixture of the components) were reduced to powder and further mixed with potassium bromide (KBr) powder. The resulting mixture was compressed into thin pellets. After that, the pellets were placed in the sample holder of the instrument and scanned in the wavelength range from  $4000$  to  $400 \text{ cm}^{-1}$  [4].

##### 2.2.2.4. Assay

TNZ content was quantified using the UV-Vis spectrophotometric method. The samples were diluted with 0.1 N HCl solution to achieve a concentration in the range of 4 to 24  $\mu\text{g/ml}$ . The absorbance was measured at the maximum absorption wavelength of 277 nm.

##### 2.2.2.5. Encapsulation efficiency

Two milliliters of TNZ-SLNs suspensions were placed in an ultrafiltration tube (Vivaspin<sup>®</sup> 6 PES, MWCO 10 kDa) and centrifuged at 5000 rpm during 15 min. Free drug was determined in the ultrafiltrate. TNZ content was measured using the described UV-Vis spectrophotometric method. The encapsulation efficiency (EE%) was calculated from the difference between the total and the free drug concentrations using the equation (1):

$$EE\% = \frac{C_{\text{total}} - C_{\text{free}}}{C_{\text{total}}} \times 100\% \quad (1)$$

Where  $C_{\text{total}}$ ,  $C_{\text{free}}$  represented the total drug and free drug concentration ( $\mu\text{g/ml}$ ) of TNZ-SLNs suspensions, respectively.

##### 2.2.2.6. In vitro drug release study

The *in vitro* drug release of TNZ-SLNs was performed using the dialysis bag diffusion technique. The samples (aqueous TNZ suspension and TNZ-SLNs suspension) (13 mg of TNZ, respectively) were placed in a dialysis bag (MWCO 12-14k Da, Visking Tubes, UK). These bags were immersed in 300 ml of PBS buffer pH 6.8 in a dissolution tester (LOGAN UDT-804, USA, using a stirring apparatus). The medium was maintained at  $37 \pm 0.5^\circ\text{C}$  under continuous stirring of 50 rpm. At predetermined intervals, aliquots of 1 ml dissolution medium were withdrawn and replaced by the same volume of fresh medium. The percentage of drug release was determined using the UV-Vis method [3, 5].

### 3. RESULTS

#### 3.1. Preparation and optimization of tinidazole - loaded solid lipid nanoparticles

##### 3.1.1. Screening of lipids

TNZ-SLNs were prepared using various lipid types, including Precirol ATO 5, GMS, and stearic acid at a concentration of 2%, while maintaining a fixed lipid-to-drug ratio of 10:1 and a Tween 80 concentration of 1.5%. The results were shown in Fig. 1.A. The results indicated that both Precirol ATO 5 and stearic acid yielded larger particle sizes (> 250 nm), whereas GMS exhibited smaller particle sizes with desired values (< 250 nm). As a result, GMS was selected as the preferred lipid carrier for the drug delivery system.

With a fixed lipid-to-drug ratio of 10:1 and a 1.5% concentration of Tween 80, an investigation was conducted on the GMS lipid concentration ranging from 1% to 3%. The results in Fig. 1.B indicated that as the lipid concentration increased from 1% to 3%, there was a tendency for the particle size to increase. The EE showed an increasing trend with lipid concentrations from 1% to 2%, but then decreased as the lipid concentration continued to increase. The range of 1 - 2% lipid concentration resulted in NPs with a high PDI (PDI > 0.5), which gradually decreased as the lipid concentration increased. The optimal lipid concentration range for further optimization was found to be between 2% and 3%.

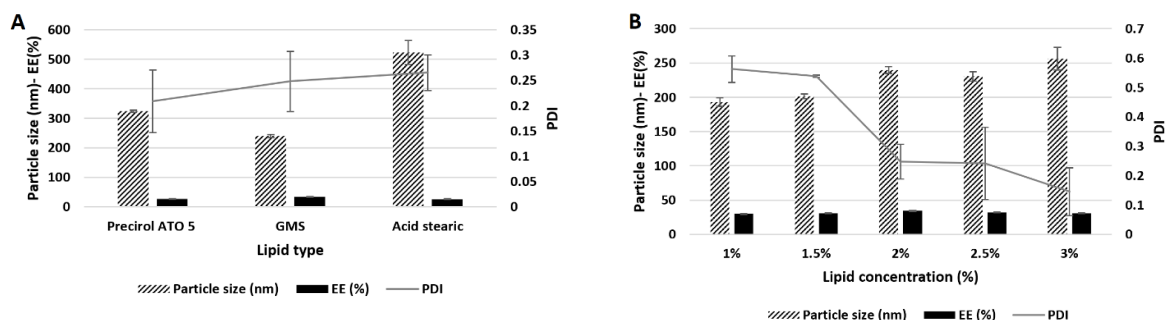


Figure 1. The effect of lipid type (A) and lipid concentration (B) on the physicochemical properties of TNZ-SLNs

##### 3.1.2. Screening of surfactants

The type of surfactant was varied at the same concentration of 1.5% while maintaining a fixed lipid-to-drug ratio of 10:1 and a 2% concentration of GMS. Based on the results in Fig. 2.A, it was observed that when using Tween 80 as the surfactant, TNZ-SLNs exhibited small particle size (< 250 nm) and narrow PDI (PDI < 0.3). Therefore, Tween 80 was chosen as the surfactant for subsequent studies.

TNZ-SLNs were prepared using varying the concentration of Tween 80 from 1.5% to 3%, while keeping the GMS concentration fixed at 2% and maintaining a lipid-to-drug ratio of 10:1. The results obtained in Fig. 2.B revealed that as the concentration of Tween 80 increased, the particle size tended to decrease, while PDI increased, and EE decreased. The concentration of Tween 80 was chosen within the range of 1.5% to 2.5% for further optimization.

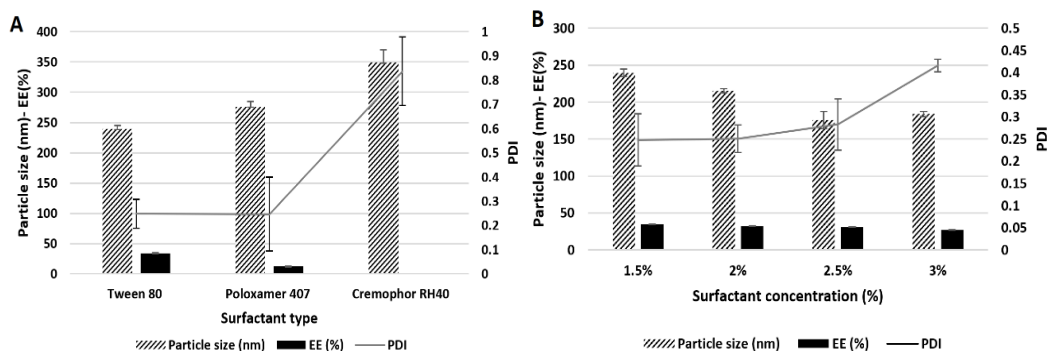
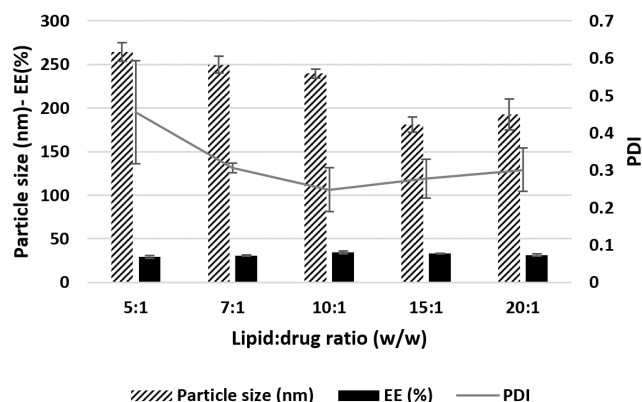


Figure 2. The effect of surfactant type (A) and surfactant concentration (B) on the physicochemical properties of TNZ-SLNs

### 3.1.3. Screening of lipid:drug ratios

The lipid-to-drug ratios between 5:1 and 20:1 were investigated for TNZ-NPs preparation by fixing the Tween 80 ratio at 1.5% and the GMS concentration at 2%. The results in Fig. 3 revealed that as the lipid-to-drug ratio increased from 5:1 to 10:1, the EE increased, while the particle size and PDI decreased. Increasing these ratios from 10:1 to 20:1, the EE decreased, but these differences were not significant. Hence, the lipid-to-drug ratios ranging from 7:1 to 20:1 were selected for further optimization.



**Figure 3.** The effect of lipid:drug ratio on the physicochemical properties of TNZ-SLNs

### 3.1.4. Optimization of tinidazole - loaded solid lipid nanoparticles

The independent and dependent variables were chosen based on the preliminary studies. Table 1 below shows their ranges of variability. The design of experiments showed 15 experimental runs, which were presented in Table 2.

**Table 1.** Variables of the optimization study

		Code	Unit	Low level	High level	Constraints
Independent variables	GMS concentration	X1	%	2	3	In range
	GMS: TNZ ratio	X2		7	20	In range
	Tween 80 concentration	X3	%	1.5	2.5	In range
Dependent variables	Particle size	Y1	nm			< 250
	PDI	Y2				< 0.300
	EE	Y3	%			Maximum

**Table 2.** TNZ-SLNs formulations based on Box–Behnken design and their measured characteristics.

Batch	X1 (%)	X2	X3 (%)	Y1 (nm)	Y2 (nm)	Y3 (%)
1	2.5	7	2.5	176.30 ± 6.50	0.284 ± 0.071	35.32 ± 0.34
2	3	13.5	2.5	221.00 ± 8.20	0.223 ± 0.032	30.60 ± 0.19
3	3	7	2	182.20 ± 4.80	0.287 ± 0.104	21.74 ± 0.25
4	2.5	7	1.5	200.20 ± 15.40	0.228 ± 0.061	31.29 ± 0.32
5	2	20	2	134.90 ± 5.40	0.333 ± 0.036	27.52 ± 0.17
6	2.5	20	2.5	223.70 ± 10.20	0.281 ± 0.017	21.60 ± 0.67
7	2.5	20	1.5	201.70 ± 6.40	0.167 ± 0.061	30.43 ± 0.29
8	2	7	2	129.40 ± 17.90	0.414 ± 0.089	36.03 ± 0.41
9	3	20	2	284.30 ± 8.90	0.114 ± 0.035	22.19 ± 0.13
10	3	13.5	1.5	181.80 ± 16.50	0.226 ± 0.041	34.76 ± 0.24
11	2	13.5	1.5	239.40 ± 16.10	0.202 ± 0.045	36.13 ± 0.32

12	2	13.5	2.5	150.50 ± 6.80	0.278 ± 0.037	24.79 ± 0.29
13	2.5	13.5	2	227.50 ± 7.10	0.190 ± 0.021	40.40 ± 0.79
14	2.5	13.5	2	235.50 ± 5.90	0.188 ± 0.028	42.36 ± 0.42
15	2.5	13.5	2	221.50 ± 10.70	0.189 ± 0.081	41.60 ± 0.36

The analysis using FormRules v2.0 software revealed a clear dependency of particle size, PDI, and EE on the input variables. The statistical analysis using InForm v3.1 software showed that the R<sup>2</sup><sub>adjusted</sub> for particle size, PDI, and EE were higher than 80% (83.73%, 91.37%, 91.79%, respectively)

Response surface analysis also shows the impact of the independent variables on the dependent variables (Fig. 4). When the X3 concentration was low and X2 increased from 7:1 to 15:1, the particle size increased. However, when X2 reached 20:1, Y1 decreased significantly. On the other hand, when X3 was high and X3 increased, Y1 showed the opposite trend. When X1 and X3 were reduced, EE increased. When X1 decreased and X2 increased, Y2 decreased.

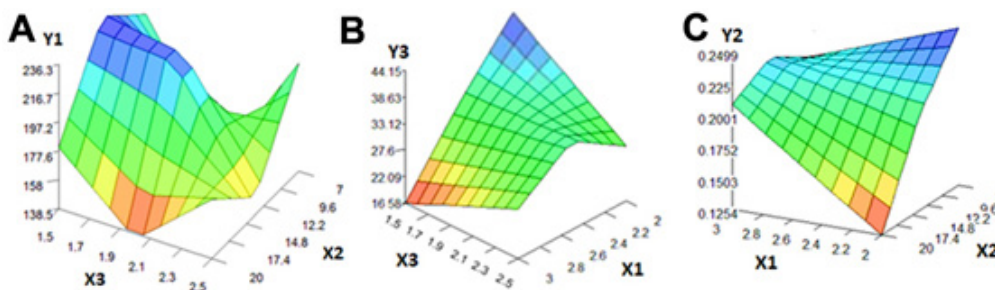


**Figure 4.** The response surface graphs showing the effect of input variables on the physicochemical properties of TNZ-SLNs: Particle size (A), EE (B), PDI (C)

The optimization of TNZ-SLNs was performed using InForm v3.1 software. For model validation, TNZ-SLNs were prepared and characterized following the optimized inputs (n = 3) (Table 3).

**Table 3.** The validity of the optimal formulation of TNZ-loaded nanoparticles

Inputs			
	X1 (%)	X2	X3 (%)
Predicted	2	13.15	1.56
Responses			
	Y1 (nm)	Y2	Y3 (%)
Predicted	208.37	0.24	39.83
Observed	197.60 ± 19.67	0.247 ± 0.011	37.96 ± 0.91
Bias*	5.17 %	2.92 %	2.63 %

$$*: \text{Bias (\%)} = \frac{|\text{Observed response} - \text{predicted response}|}{\text{predicted response}} \times 100$$

It was observed that the deviations were low, especially less than 5% for Y2 and Y3, indicating the validity of generated models without the significant difference between the predicted and the actual results. In addition, the optimized formulation had the zeta potential of -15.79 ± 0.75 mV.

### 3.3. Physicochemical characterization of tinidazole – loaded solid lipid nanoparticles

#### 3.3.1. X-ray diffraction analysis

The XRD spectra of the samples (Fig. 5.A) exhibited distinct peaks in the diffraction pattern of the drug compound, indicating its crystalline state. Sharp peaks corresponding to the drug compound were observed at 2θ angles of 17.69°, 18.19°, 22.32°, and 23.72°. The XRD pattern of GMS showed peaks at 2θ angles of 19.44°, 20.42°, 21.61°, and 23.03° [6, 7]. The characteristic peaks of the drug compound and GMS had either disappeared or reduced in intensity in the XRD spectrum of TNZ-SLNs. This suggested that the drug compound was present in an amorphous state or had been uniformly dispersed within the lipid layer of

NPs. The amorphous state of the drug compound enhanced its solubility, contributing to an increased bioavailability of the formulation.

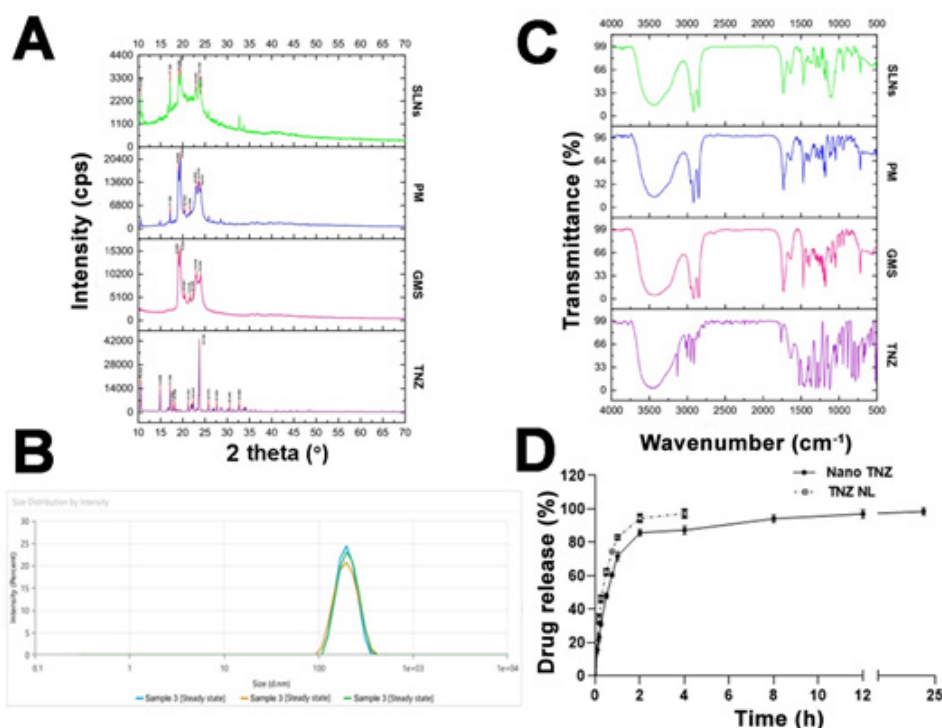


**Figure 5.** (A) XRD patterns, (B) Particle size of TNZ-SLNs, (C) FT-IR spectra of TNZ, GMS, TNZ-SLNs, physical mixture (PM), and (D) The *in vitro* drug release study of aqueous TNZ suspension and TNZ-SLNs suspension in pH 6.8 (n = 3)

### 3.3.2. Fourier Transform-Infrared (FTIR) spectroscopy analysis

The functional groups present in the samples were determined using infrared spectroscopy (Fig. 5.C). The spectrum of TNZ-SLNs matched well with the individual spectra. The TNZ spectrum exhibited several intense peaks at 1301 cm<sup>-1</sup> (corresponding to the asymmetric stretching of S=O), 1523 cm<sup>-1</sup> (corresponding to the C=N vibration of the imidazole ring) (Fig. 5.C) [7]. The GMS spectrum showed characteristic peaks at 1105 cm<sup>-1</sup> (C-O-C stretching), 1730 cm<sup>-1</sup> (-C=O of GMS), 2850 cm<sup>-1</sup>, and 2920 cm<sup>-1</sup> (corresponding to C-H in long-chain CH<sub>2</sub> groups). Most of the absorption peaks of the raw drug compound decreased in intensity upon the formation of TNZ-SLNs. The presence of these absorption peaks confirms the presence of TNZ in TNZ-SLNs. The overlapping spectra results demonstrated that neither NPs nor the PM exhibited any additional peaks apart from those of GMS and TNZ, indicating no chemical interaction between the components during the preparation process. Compared to the PM

sample, the vibrational peaks of NPs were relatively reduced, possibly due to the dominance of GMS peaks over TNZ when in a homogeneously distributed molecular state.

### 3.3.3. In vitro drug release study

The *in vitro* drug release of TNZ-SLNs suspension and aqueous TNZ suspension were presented in Fig. 5D. The results showed that the drug release from TNZ-SLNs underwent two distinct and prominent stages, with a substantial release during the first 2 hours (85.84 ± 0.91%) followed by a gradual release over the remaining 22 hours. This result showed the potential for developing sustained-release drug formulations containing TNZ.

## 4. DISCUSSION

The SLNs utilizing different lipid matrices exhibited diverse characteristics, as each lipid possessed a distinct structure, composition, and physical properties. This study evaluated the effect of formulation factors on several properties of TNZ-SLNs.

The research results demonstrated that the use of

stearic acid generates NPs with a higher particle size (>500 nm), while GMS and Precirol produce smaller particle sizes (<350 nm) and higher EE compared to stearic acid. This difference could be attributed to variations in the melting temperature among the lipids, as particle size tended to increase when lipids with higher melting points were used [8]. Stearic acid had a melting point of 69–70 °C, which was higher than that of Precirol ATO5 (50–60 °C) and GMS (55–60 °C), resulting in larger particle sizes for stearic acid compared to GMS and Precirol. Additionally, GMS served as both a matrix-forming lipid and an emulsifier, which explained its smallest particle size. In terms of EE, the difference between these two types of lipids may be due to their distinct crystalline states. GMS and Precirol exhibited a disordered crystalline state, creating more void spaces to accommodate drug molecules and consequently enhancing the EE. On the contrary, stearic acid had a highly ordered crystalline state, leading to decreased EE. This finding was consistent with the study conducted by Jennings V. et al. [9]. The research revealed that GMS provided the best results among the investigated lipids. GMS functioned as a matrix-forming lipid and had emulsifying capabilities with an HLB value of 3.8 [10]. GMS had also been widely used as a matrix-forming lipid in previous studies by Kraissit P. et al. [11] and Bhalekar M. R. et al. [12].

The proper selection of surfactants prevented particle aggregation and stabilized NPs. An excessive amount of surfactant was initially needed during the preparation to quickly cover the freshly produced particle surfaces during homogenization. The particles with exposed lipid surfaces may aggregate because of insufficient surfactant concentration. The redistribution time of surfactant between the newly formed surface molecules and micelles varied with different surfactants. Generally, surfactants with lower molecular weights required less time for redistribution. This study demonstrated that different surfactants resulted in significant differences in the system characteristics. Cremophor RH40 produced NPs with larger particle sizes (>300 nm) and high PDI, indicating a broad distribution of particle sizes and poor stability. Poloxamer generated NPs with the particle size above 250 nm and low EE, whereas TNZ-SLNs prepared with Tween 80 exhibited favourable characteristics (particle size of  $239.70 \pm 5.20$  nm, low PDI), and high EE.

The particle size and EE in SLNs tended to improve with increasing lipid amounts. This might be explained by the system's increased viscosity as the lipid concentration increased. Hence, oil-in-water

emulsion droplet was poorly dispersed under the same ultrasonic energy, resulting in greater particle size in both the emulsion droplets and resulting SLNs. Increasing the lipid concentration from 1% to 2% led to an increase in EE. This might be due to the greater lipid concentration, which produced a less ordered crystalline state. Hence, this would improve drug molecule retention in NPs and subsequently, increase EE of NPs. However, EE was decreased when the lipid concentration was raised up to 3%. This might be explained by the excessive lipid concentration, which may have disturbed the normal structure of SLNs. These findings were consistent with the research of Mahmoud R.A. et al. [13].

As a result of lowering the lipid-to-drug ratio from 20:1 to 10:1, the particle size and EE was increased. When the drug concentration was increased, a larger amount of drug could be accommodated inside the lipid matrix, resulting in a better EE. The particle size continued to be grown while EE was decreased when the ratio was further dropped to 5:1. This could be due to a high concentration of drug, exceeding the lipid's ability to encapsulate drug molecules and leaving more free drugs in the external phase [14].

The surfactant concentration significantly influenced the particle size. Increasing the surfactant concentration helped reduce the surface tension and prevent molecular aggregation during the emulsification process, resulting in smaller particle size. When Tween 80 concentration was increased from 1.5% to 3%, the particle size and PDI were increased, and EE% was decreased. This could be explained that the interfacial tension between the two phases were gradually decreased during the emulsification process, preventing the growth of larger particles. However, there was a trend toward a lower EE, which may have led to greater drug solubility in the exterior phase. The investigation carried out by Chokshi, N. V., et al. was consistent with these findings [14].

The optimized formulation obtained from InForm v3.1 showed a close prediction to the actual results, with a deviation of less than 5% for most variables. Although the bias was 5.17% for particle size (higher than 5%), the actual value of particle size was lower than the predicted value and below 250 nm as the desired value. The  $R^2_{\text{adjusted}}$  were consistently above 80%, indicating that the artificial neural network accurately described the relationship between the independent and dependent variables.

In this study, some experimental softwares were applied to design and optimize SLNs, including Design Expert 12.0 software used to design

experimental formulations, FormRules 2.0 used for generating “IF...THEN” rules, and InForm 3.1 for the optimization process.

Furthermore, the Fourier-transform infrared spectroscopy (FTIR) and X-ray diffraction (XRD) patterns showed that TNZ was suffered a change in SLNs from a crystalline state to an amorphous or molecularly dispersed form. There was no proof that TNZ and excipients had chemical interaction.

According to *in vitro* drug release, the raw TNZ material displayed a rapid release, with about 100% drug released in 4 hours. Whereas TNZ-SLNs demonstrated a prolonged drug release profile with a duration of 24 hours. These findings indicated that TNZ-SLNs had modified the drug release profile compared to TNZ material.

Both lipid-based NPs and polymeric NPs can incorporate both lipophilic and hydrophilic drugs. However, in comparison with polymeric NPs, lipid-based NPs are less harmful because of their

biocompatible and biodegradable constituents and lack of any organic solvents during manufacturing and capable of producing on large industrial scale [15].

## 5. CONCLUSION

TNZ-SLNs were successfully prepared using a hot homogenization and solvent evaporation method. The optimized formulation exhibited a particle size of  $197.60 \pm 19.67$  nm, a low PDI of  $0.247 \pm 0.011$ , a zeta potential of  $-15.79 \pm 0.75$  mV, and a high EE of  $37.96 \pm 0.91\%$ . Furthermore, TNZ-SLNs demonstrated a prolonged drug release profile, with a release duration for up to 24 hours. This result highlighted the potential for developing sustained-release drug formulations of SLNs containing TNZ.

## ACKNOWLEDGMENT

This research was funded by Vietnam Ministry of Education and Training of Vietnam (MOET) under Grant no. B2022-DHH-19.

## REFERENCES

1. Alou L, Giménez M, Manso F, Sevillano D, Torrico M, González N, et al. Tinidazole inhibitory and cidal activity against anaerobic periodontal pathogens. *International journal of antimicrobial agents*. 2009;33(5):449-52.
2. Basudan AM. Nanoparticle based periodontal drug delivery-A review on current trends and future perspectives. *The Saudi Dental Journal*. 2022.
3. Ho HN, Laidmäe I, Kogermann K, Lust A, Meos A, Nguyen CN, et al. Development of electrosprayed artesunate-loaded core-shell nanoparticles. *Drug development and industrial pharmacy*. 2017;43(7):1134-42.
4. Ho HN, Do TT, Nguyen TC, Yong CS, Nguyen CN. Preparation, characterisation and *in vitro/in vivo* anticancer activity of lyophilised artesunate-loaded nanoparticles. *Journal of Drug Delivery Science and Technology*. 2020;58:101801.
5. Ho HN, Le HH, Le TG, Duong THA, Ngo VQT, Dang CT, et al. Formulation and characterization of hydroxyethyl cellulose-based gel containing metronidazole-loaded solid lipid nanoparticles for buccal mucosal drug delivery. *International Journal of Biological Macromolecules*. 2022;194:1010-8.
6. Samanta HS, Ray SK. Controlled release of tinidazole and theophylline from chitosan based composite hydrogels. *Carbohydrate polymers*. 2014;106:109-20.
7. Khan G, Yadav SK, Patel RR, Kumar N, Bansal M, Mishra B. Tinidazole functionalized homogeneous electrospun chitosan/poly ( $\epsilon$ -caprolactone) hybrid nanofiber membrane: Development, optimization and its clinical implications. *International journal of biological macromolecules*. 2017;103:1311-26.
8. Ahmed TA, Badr-Eldin SM, Ahmed OA, Aldawsari H. Intranasal optimized solid lipid nanoparticles loaded in situ gel for enhancing trans-mucosal delivery of simvastatin. *Journal of Drug Delivery Science and Technology*. 2018;48:499-508.
9. Jennings V, Gohla S. Comparison of wax and glyceride solid lipid nanoparticles (SLN®). *International journal of pharmaceuticals*. 2000;196(2):219-22.
10. Rowe RC, Sheskey P, Quinn M. *Handbook of pharmaceutical excipients: Libros Digitales-Pharmaceutical Press*; 2009.
11. Kraissit P, Yonemochi E, Furuishi T, Mahadlek J, Limmatvapirat S. Chitosan film containing antifungal agent-loaded SLNs for the treatment of candidiasis using a Box-Behnken design. *Carbohydrate Polymers*. 2022;283:119178.
12. Bhalekar MR, Madgulkar AR, Desale PS, Mariam G. Formulation of piperine solid lipid nanoparticles (SLN) for treatment of rheumatoid arthritis. *Drug development and industrial pharmacy*. 2017;43(6):1003-10.
13. Mahmoud RA, Hussein AK, Nasef GA, Mansour HF. Oxiconazole nitrate solid lipid nanoparticles: formulation, *in-vitro* characterization and clinical assessment of an analogous loaded carbopol gel. *Drug development and industrial pharmacy*. 2020;46(5):706-16.
14. Chokshi NV, Khatri HN, Patel MM. Formulation, optimization, and characterization of rifampicin-loaded solid lipid nanoparticles for the treatment of tuberculosis. *Drug development and industrial pharmacy*. 2018;44(12):1975-89.
15. Kahraman E, Gungor S, Ozsoy Y. Potential enhancement and targeting strategies of polymeric and lipid-based nanocarriers in dermal drug delivery. *Ther Deliv*. 2017;8(11):967-85.